Adv. Space Res. Vol. 1, pp.127-141. 0273-1177/81/0301-0127$05.00/0

MEASUREMENT OF MINOR SPECIES (H_2, Cl, O_3, NO) IN THE EARTH'S ATMOSPHERE BY THE OCCULTATION TECHNIQUE

S. K. Atreya

Department of Atmospheric and Ocean Science, Space Physics Research Laboratory, The University of Michigan, Ann Arbor, Michigan 48109, USA

1. ABSTRACT

The stellar occultation technique is a clean and powerful means of detecting and quantifying minor gases in the earth's atmosphere. The results obtained are totally insensitive to knowledge of the absolute flux of the star, and are not influenced by instrument calibration problems. Pioneering observations of nocturnal mesospheric ozone and thermospheric molecular oxygen by the stellar occultation technique were made in 1970 and 1971 with the Wisconsin stellar photometers on board the Orbiting Astronomical Observatory-2. A limb crossing geometry was used. The high resolution Princeton ultraviolet spectrometer aboard Copernicus was used in the summers of 1975, 1976 and 1977 to measure altitude profiles of molecular hydrogen, atomic chlorine and nitric oxide in addition to ozone and molecular oxygen. A limb grazing geometry was employed. The ozone densities show wide variation from orbit to orbit and particularly between the OAO-2 and Copernicus observations. A H_2 density of 1×10^8 cm^{-3} at 95 km, and a NO density less than 10^6 cm^{-3} for altitudes greater than 85 km were measured.

2. INTRODUCTION

In a stellar occultation, the atmosphere of earth acts as a large absorption cell through which light from a stellar source is attenuated. Knowing the identity and absorption characteristics of the gases in this medium, one can determine the line of sight column abundance and subsequently the vertical number density of the absorbers independent of knowledge of the absolute stellar flux. The stellar occultation technique is a powerful means of determining nighttime altitude distributions of minor species in the earth's atmosphere. Unlike solar occultations, the above technique does not suffer from the problem of poor height resolution. For normal satellite altitudes, the angular diameter of the sun, 0.5° at 1 AU, results in a 25 km averaging over height in the mesosphere. The stellar occultation technique has been able to yield vertical height resolution on the order of few hundred meters.

The stellar occultation technique was first analyzed by Pannekoek [1] to discern composition and structure of planetary atmospheres. Baum and Code [2] used the technique to determine Jovian mesospheric temperatures by occultation of visible light from σ-Arietis. The first successful application of the stellar occultation technique to the terrestrial atmosphere was made by Hays and Roble in 1970 and

1971, using the Wisconsin stellar photometers aboard the Orbiting Astronomical Observatory, OAO-2. Using an OAO-2 filter centered at 1500Å, Hays et al [3] and Hays and Roble [4] determined the O_2 density between 120 and 200 km by studying absorption of stellar light in the O_2 - Schumann - Runge continuum. Use of the OAO-2 filters centered at 2390Å and 2460Å enabled them to measure the O_3 density between 60 and 100 km.

The high spectral resolution of the Princeton ultraviolet spectrometer aboard Orbiting Astronomical Observatory 3 - Copernicus provided an unprecedented opportunity of detecting and measuring species even less abundant than ozone. Riegler et al [5, 6], Atreya et al [7], and Atreya et al [8] carried out numerous stellar occultation exercises on Copernicus to measure Cl, H_2, and NO in addition to O_3 and O_2 in the mesosphere and thermosphere. The Copernicus observations used a 'limb grazing' geometry rather than the conventional 'limb crossing' geometry employed in OAO-2 observations. In the latter geometry the line of sight to the star crosses the limb of the earth in 10 to 20 seconds depending upon the satellite altitude. In the limb grazing geometry, on the other hand, the line of sight to the star grazes the earth's limb in 200-300 seconds without being actually occulted by it. Consequently, the Copernicus observations yield extremely good statistics and slow rate of change of tangent ray height.

This paper provides an overview of the observations of terrestrial minor gases by the stellar occultation technique. The shortcomings of the technique are discussed, and the potential for future observations of significant trace species by such spacecraft as IUE and ST is explored.

3. OBSERVATION AND INVERSION TECHNIQUE

The geometry of stellar occultation is shown in Figure 1 for a spherically strati-

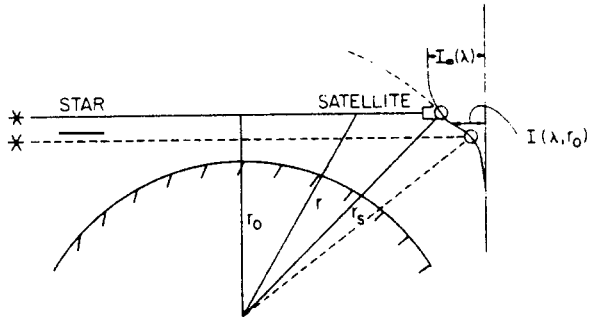

Fig. 1 Geometry of an ultraviolet stellar occultation (Hays et al [3]). $I_\infty(\lambda)$, and $I(\lambda, r_0)$ are unattenuated counting rates and counting rate at tangent altitude r_0 at wavelength λ.

fied atmosphere. When ultraviolet light from a star (source) passes well above the atmosphere the spectrometer (detector) on board the satellite measures an unattentuated count rate $I_\infty(\lambda)$ at a given wavelength. As the spacecraft moves in its orbit, the line of sight to the star traverses denser atmospheric layers, and light is attentuated to $I(\lambda, r_o)$ due to absorption by gases in the atmosphere (cell). The two intensities are related by Beer's law:

$$I(\lambda, r_o)/I_\infty(\lambda) = \exp\left[-\sum_i \tau_i\right] \tag{1}$$

where

$$\tau_i = \sigma_i(\lambda) \cdot N_i(r_o) \tag{2}$$

is line of sight optical depth of i^{th} species whose absorption cross section at wavelength λ is $\sigma_i(\lambda)$, and whose line of sight (tangential) column abundance at tangent ray height r_o is $N_i(r_o)$.

For a spherically stratified atmosphere, one can write, after Hays and Roble [9]

$$N_i(r_o) = 2\int_{r_o}^{\infty} \frac{n_i(r)\, r\, dr}{(r^2 - r_o^2)^{1/2}} \tag{3}$$

where $n_i(r)$ is vertical number density of i^{th} specie at tangent ray height r. Equation (3) may be inverted by the numerical iterative technique used by Atreya et al [7], or by the Abel inversion technique as described by Hays and Roble [9] to yield $n_i(r)$.

$$n_i(r) = \frac{d}{dr}\left[-\frac{1}{\pi}\int_r^{\infty} \frac{r}{r_o} \frac{N_i(r_o)\, dr}{(r_o^2 - r^2)^{1/2}}\right] \tag{4}$$

The above technique for determining $n_i(r)$ depends only on the ratio of $I(r_o)/I_{(\infty)}$, equation (1). The results are, therefore, independent of the absolute stellar flux. The accuracy of the results is greatly improved by use of a star which has continuum flux at the selected wavelength, and when one is dealing primarily with a single absorber.

4. OBSERVATIONS OF H_2, O_2 AND Cl

Measurements of terrestrial H_2 and Cl were made using the Princeton ultraviolet spectrometer on board OAO-3 - Copernicus. The O_2 density measurement is a by-product of the H_2 observations. The Copernicus satellite is in near-circular orbit of 745 km altitude and 25° inclination. These orbital parameters permit long occultation periods during each orbit and allow one to make long term predictions of future occultation targets and times. The Copernicus star tracker tracks on a portion of the visible light entering the telescope while the other portion is directed to the UV spectrometer. The use of visible light in the star tracker, and UV light in the spectrometer leads to refraction effects and possible guidance problems which restrict useful occultation geometry to tangent altitudes greater than 47 km. The star tracker design and other engineering constraints limit viewing to within three hours of local midnight at the tangent point. These factors along with the choice of limb grazing method reduce occultation opportunities to one or two stars per year.

The first successful measurement of H_2 was carried out by Atreya et al [7] using a bright star - γ^2 Velorum (HD 68273; type: O; V = 1.83) which has a continuum flux of about 3000 photons cm^{-2} s^{-1} $Å^{-1}$ in the UV at 1100Å. Since the volume mixing ratio of H_2 at 100 km is on the order of 10^{-6} according to model calculations by Liu and Donahue [10, 11, 12], and since continuum and band absorption by H_2 occurs in the spectral range where O_2 also absorbs strongly, all previous attempts (see, e.g., paper by Feldman and Takacs [13]) to measure it either in resonance-fluorescence or in absorption spectroscopy failed.

The principle of the Copernicus H_2-experiment is to detect H_2 in absorption at a wavelength where the H_2-line of sight optical depth is comparable to or exceeds the O_2-optical depth in the same line of sight. An examination of the oscillator strengths and spectral structure of all rotational-vibrational lines of H_2 in its Lyman and Werner band system revealed that the above criterion was satisfied only at 1108.128Å, 1094.244Å, and 1077.138Å since there are deep minima in the O_2 absorption spectrum in the immediate vicinity of these lines of H_2. For these calculations, the H_2 density at 100 km was taken to be $5x10^7$ cm^{-3} according to Liu and Donahue [10, 11, 12], and the positions, of H_2 rotational-vibrational line centers and corresponding oscillator strengths were taken from Morton and Dinerstein's [14] compilation.

In 1976-Copernicus observations the region near 1108Å was selected (Fig. 2).

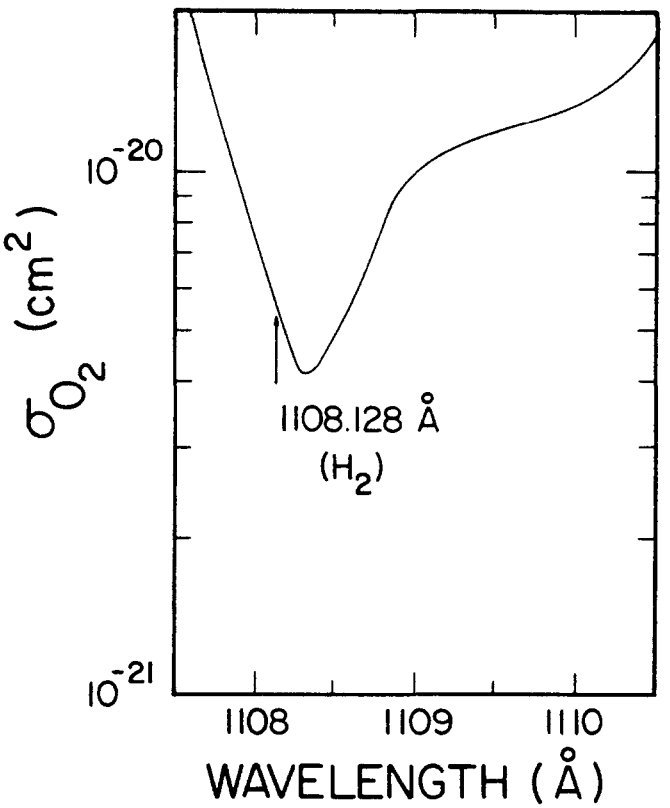

Fig. 2 Absorption cross section of O_2 in the vicinity of the R(0) line of H_2 Lyman band at 1108.128Å.

At the R(0) line of the (0, 0) Lyman absorption band at 1108.128Å, The H_2 oscillator strength is 0.00173, and the total absorption cross section of O_2 is taken to be 5.4×10^{-21} cm^2 from Watanabe's [15] compilation. The unattentuated stellar flux was monitored over a few dozen Copernicus orbits, and no spectral signature (other than continuum) in the vicinity of 1108Å was detected. The high resolution spectrometer tube U1 which has a bandpass of 0.04Å at 1108Å was positioned three wavelength steps, $3\Delta\lambda$, (where $\Delta\lambda$ = 0.022Å) to the blue side of the selected R(0) line of H_2. Thus, for the leftmost position the spectrometer bandpass was completely outside the line profile of R(0) line which has a spectral half width of 0.0078Å at 200 K. The spectrometer position was moved by $\Delta\lambda$ in each orbit of the satellite so that in the fourth orbit the R(0) line centered at 1108.128Å was entirely within the instrument bandpass. The spectrometer was moved by one more $\Delta\lambda$ in the following orbit to detect the variation in counting rates due to increased O_2 absorption. We show the data of orbit 1 and 4 in Figs. 3 and 4. The counting rates integrated at the end of each 14 sec interval are

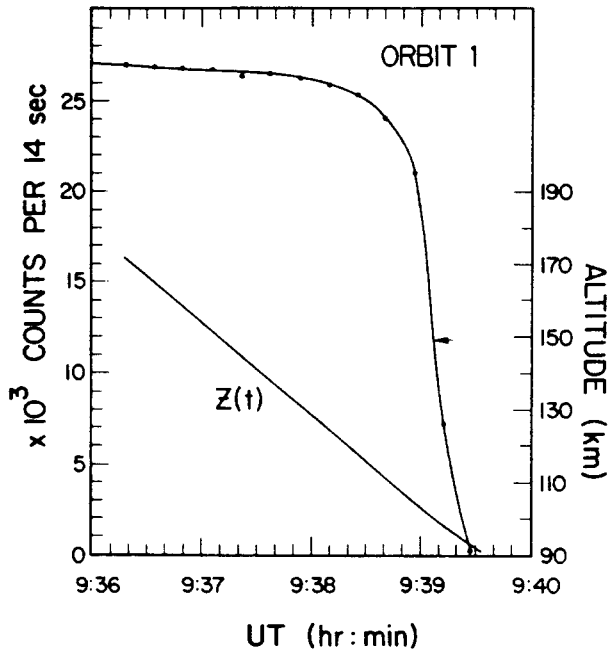

Fig. 3 The variation of count rates as a function of the universal time for orbit 1. A temporary reduction in the count rate at $9^h37^m\ 22^s$ is due to a guidance error. The variation of the tangent altitude during this observation is shown as a function of the universal time by the curve labeled Z(t). The minimum tangent altitude in this orbit was 50.9 km. The count rate at 100 km is marked with an arrow. Atreya et al [7].

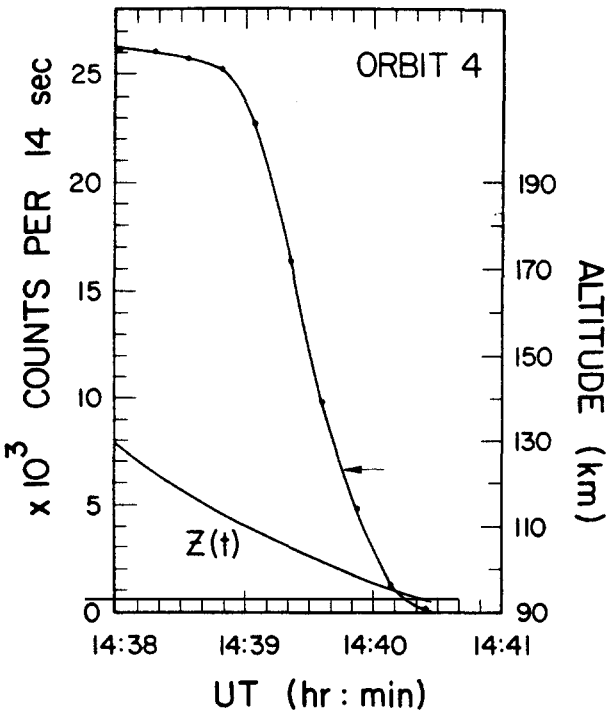

Fig. 4 Same as Figure 1 except for orbit 4. The minimum tangent altitude in this orbit was 85.8 km. Atreya et al [7].

shown as a function of time in orbit. The corresponding variation of tangent ray height is shown by the curves marked Z(t). The data have been corrected for dark count; the primary cause for noise is cosmic ray-induced photo-events. The smoothing and interpolation of the data are carried out by cubic spline fit, logarithmic fit and least squares method.

A comparison of the counting rates in orbits 1 and 4 (Figs. 3 and 4) indicates a large depletion of count rates below 110 km. For example, the horizontal arrows in Figs. 3 and 4 show that the counting rate at 100 km in orbit 4 is only half that in orbit 1, presumably due to onset of H_2-absorption. (In order to find counting rate at a given altitude: find time, t for the desired altitude, Z using curve Z(t); now read counting rate corresponding to this time using counting rate vs UT curve.) The data of orbit 1 can be directly used to discern the O_2 density profile using the inversion techniques described in Sec. 3. The results are shown in Figure 5. For comparison, we also show the Jacchia [16] equatorial model O_2 densities for 900K exospheric temperature - these conditions being quite representative of the epoch of the Copernicus H_2-observations.

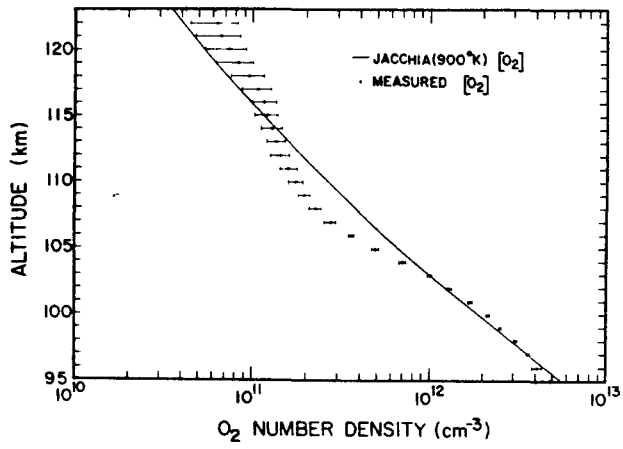

Fig. 5 The measured O_2 densities and associated error bars. The Jacchia [16] model (900K) O_2 density profile is shown by the solid line curve. Atreya et al [7].

One finds a reasonably good fit between the data and the model. A wavelike structure in the data is reminiscent of the propagation of inertia gravity waves, as has been noted also in the OGO-6 data (Donahue, T. M., personal communication, 1980). The actually measured line of sight optical depth of O_2 (from orbit 1) and Rayleigh scattering effects were subtracted from the total measured optical depth at each altitude in orbit 4. Thus, any uncertainty in the O_2 absorption cross section does not affect the results. The remaining optical depth is due to H_2-absorption.

The H_2-densities for J = 0 line between 95 and 108 km are then determined by the same inversion techniques as used for O_2. Knowing the population in the J = 0 level, one can determine the total H_2 abundance provided that the temperature profile in the 95-108 km is also known. We show in Fig. 6 the population distribution for various rotational levels at 200 K, 250 K, and 300 K. The inset in Fig. 6 shows percentage population in J = 0 level for various assumed temperature profiles. The resultant total H_2 density profile is shown in Figure 7 for various assumed temperature profiles. The uncertainty in the determination of density is about 5% at 95 km and it increases to 35% at 108 km due to vanishing optical depth of H_2. Figure 7 also shows the range of theoretical calculations by Liu and Donahue [10, 11, 12]. The best fit to the data is obtained when the high value of the rate constant, k in the following H_2-production mechanism is used:

$$H + HO_2 \xrightarrow{k} H_2 + O_2 \tag{5}$$

$$\text{where } k = 1.3 \times 10^{-11} \exp(-330/T) \tag{6}$$

The above measurements of H_2 describe a new technique for detecting minor species which are obscured by dominant gases with overlapping absorption characteristics.

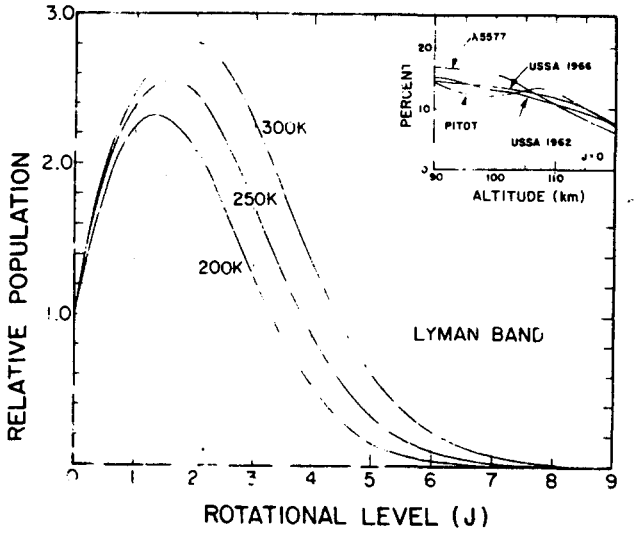

Fig. 6 Relative populations of various rotational levels at 200K, 250K, and 300K. The inset shows percentage populations in J=0 state as a function of height corresponding to the US Std. Atmosphere 1962, 1966; λ5577, and Pitot Tube (Donahue and Carignan [17]) temperatures.

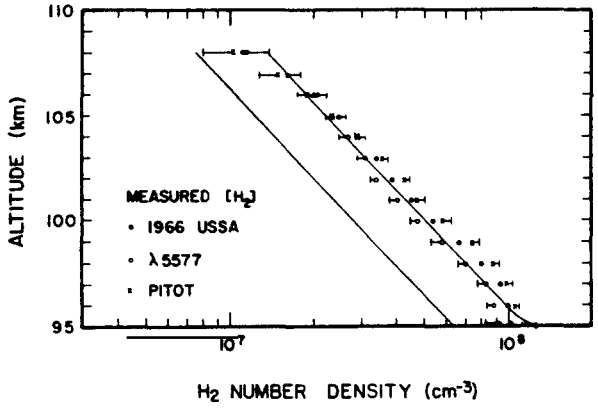

Fig. 7 The H_2 densities as deduced from the inversion of the orbits 4 and 1 data. The densities are plotted for the various assumptions of the temperature profiles discussed in the text. The negative error bar is placed on the lowest H_2 density while the positive error bar on the highest density at each altitude. The range of Liu and Donahue ([10], [11], [12]) models, discussed in the text, is shown by the solid line curves. Atreya et al [7].

The same technique was also used to detect chlorine by Riegler et al [6]. The search for Cl was made at a ground state transition of atomic chlorine at 1188.775Å. This feature lies in the minimum of O_2-absorption cross section near 1187Å. Occultation of another bright star β Centauri A (HD122451, B1 III, V = 0.62) was studied. The technique of observations and data inversion was similar to the H_2-observations. Figure 8 shows a spectral scan in the vicinity of 1188Å feature.

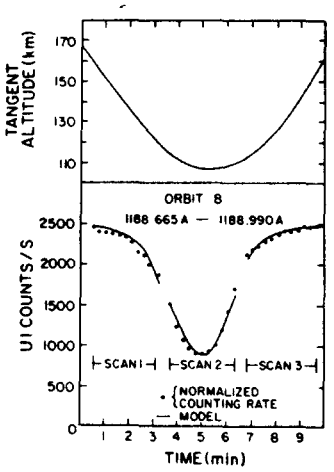

Fig. 8 (Top) Viewing geometry as a function of time. (Bottom) Dots denote the observed counting rates for three spectral scans near the 1188-Å line of atomic chlorine. The solid line illustrates one sample fit to the data points, when absorption along the line of sight due to molecular oxygen only is assumed. Riegler et al [6].

These observations provided an upper limit to the Cl abundance of $1x10^4$ cm^{-3} which corresponds to a $3x10^{-9}$ mixing ratio at 106 km, assuming the appropriate atmospheric model for the observation geometry and times. This upper limit of Cl exceeds the theoretical prediction (S. C. Liu, personal communication, 1976) by up to a factor of 2.5.

5. OBSERVATIONS OF O_3

Unlike the H_2 and Cl measurements discussed in Sec. 4, the O_3 measurements are considerably simpler to make, due to the fact that in the Hartley continuum, other than O_3, only small contributions to optical depth due to Rayleigh scattering need be considered. Since O_3 is the dominant absorber in this spectral region, one is, therefore, not constrained to work in only a few specific narrow (<1Å) regions like in H_2 and Cl observations. This is particularly true of wavelengths longward of 2400Å. Hays and Roble [4] first applied the stellar occultation technique to measure ozone in the 60-100 km range using the OAO-2 filters centered at 2390Å and 2460Å. Studying occultations of several bright stars over 12 OAO-2 orbits, they deduced the nightside O_3 density in the mid-and equatorial latitudes. Unlike the observations of Hays and Roble [4], Riegler et al [5, 6] and Atreya, Donahue and Riegler [8] employed a limb grazing geometry

(see Section 2) thus substantially improving the statistics and lower the rate of change of tangent ray altitude. The latter authors carried out their observations using high resolution spectrometers V1 and V2 on Copernicus. The high spectral resolution of the spectrometer ensures a high degree of accuracy in the retrieved data by eliminating effects of possible features in the stellar spectrum and of averaging absorption cross sections of O_3 and O_2 over the instrument bandpass. Hays and Roble measured the O_2 density from 120 km to 200 km simultaneously with all their O_3 observations, while only two of the Copernicus orbits had simultaneous O_2 measurements. A synopsis of all stellar occultation measurements of O_3 to date is presented in Table 1. All observations were for equatorial latitudes with the exception of a few OAO-2 orbits which yielded data on mid-latitude ozone.

TABLE 1 Synopsis of Stellar Occultation Measurements of O_3

Date	Stars Occulted	Number of Useful Orbits	Wavelength of Observations (Å)	Spectral Resolution (Å)	Altitude Range (km)	References
8/70, 12/70 and 9/71	α And β lup, δ, τ Sco γ Peg, i Her	12	2390 and 2460		60-100	Hays et al [3] and Hays and Roble [4]
7/75	β Cen A	4	2580, 2825, 2997, and 3100	0.06-0.08	47-114	Riegler et al [6]
6/76	β Cen A	8	2550, 2700, 2900, 3000, and 3100	0.4	47-114	Riegler et al [5]
7/77	β Cen A	9	2522, 2900, 3041, 3100	0.06-0.08	47-114	Atreya, Donahue and Riegler [8]

Typical viewing geometry and counting rate as a function of time are shown in Fig. 9, taken from the 1975 Copernicus observations. The retrieved line of sight O3 column densities for 1975 and 1976 Copernicus observations are shown in Fig. 10. The local vertical densities for individual orbits of 1976 observations deduced in the manner described in Sec. 3 are shown in Fig. 11. In order not to clutter the figures with all the data, the ranges of 1975 and 1976 O_3 densities along with results of individual orbits of 1977 Copernicus observations are plotted in Fig. 12. Note that other than orbit 4, all other 1977 densities fall in the same range as the 1975 and 1976 values. The minimum at 85 km does appear to be more pronounced in 1977. We also show in this figure the range of equatorial O_3 densities from OAO-2 data of Hays and Roble [4].

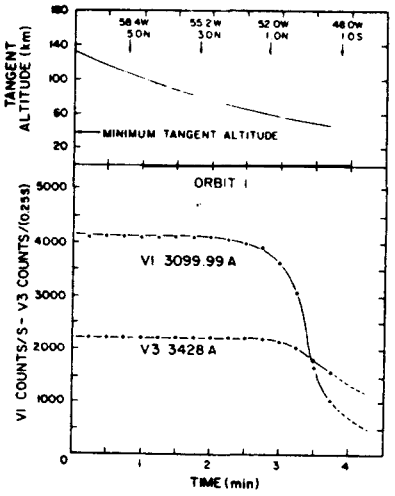

Fig. 9 Viewing geometry and counting rates observed during ozone absorption measurements on orbit 1. Riegler et al [6].

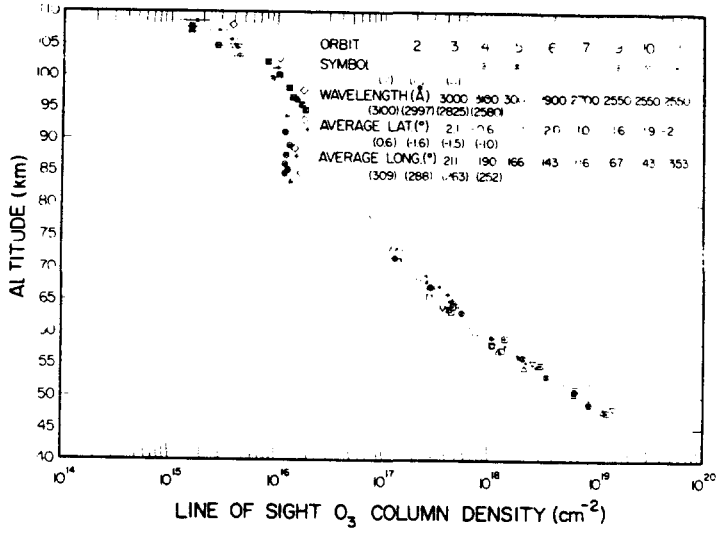

Fig. 10 Line of sight ozone column density from the 1975 and 1976 stellar occultation measurements of β Cen. Wavelengths and average latitudes and longitudes shown in the parenthesis are for the 1975 observations. Error bars of one standard deviation length are shown only when the error exceeds 10%. Riegler et al [5].

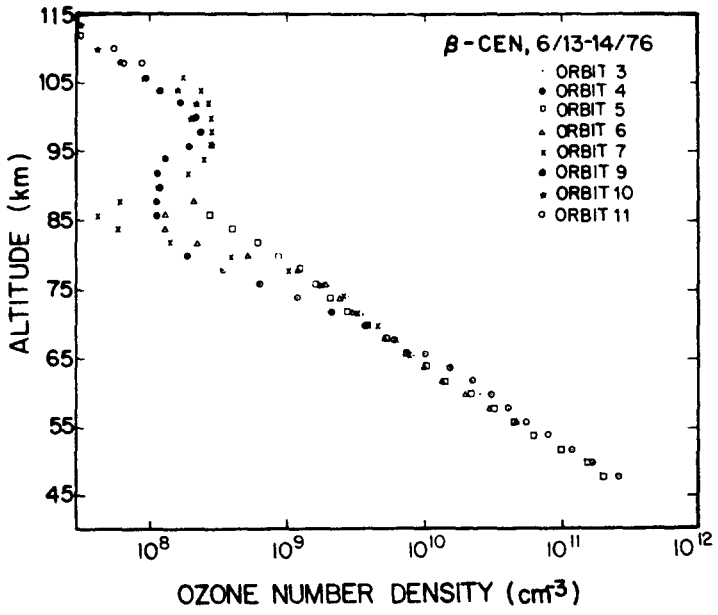

Fig. 11 O_3 vertical number densities deduced from absorption data of each of the 1976 Copernicus orbits 3, 4, 5, 6, 7, 9, 10, and 11.

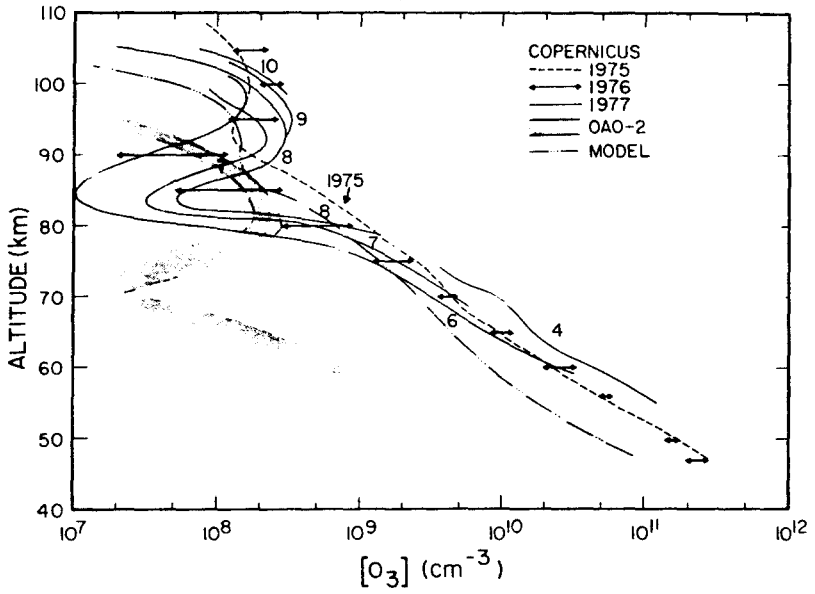

Fig. 12 Comparison of 1975, 1976, and 1977 Copernicus, and 1971-1972 OAO-2 observations of O_3. The mean of 1975 observations (4 orbits) and range of 1976 observations are shown alongside results of individual 1977 observations. The model calculations are due to S. C. Liu and T. M. Donahue.

The LRIR measurements of Gille et al [18] carried out on the night before the 1975 Copernicus observations and for the same latitude give O_3 densities a factor of 2 to 3 lower between 50 and 65 km. The Gille et al [18] measurements, on the other hand, do not agree with any other nighttime equatorial O_3 data. A recent one dimensional theoretical model by Liu and Donahue (personal communication, 1980) for midnight equatorial conditions is also given in Figure 12.

One finds a wide discrepancy between the results of various observations and the model. One should note that the OAO-2 observations were done near solar maximum while the Copernicus observations were near solar minimum. Since the Copernicus values are generally greater by a factor of 2 to 3 than the model predictions and daytime observations made by Krueger and Minzner [19], a logical argument could be made that the tangent ray height calculations may have been in error by 4 to 5 km. A thorough repetition of the ephemerides, spacecraft attitude data and orbital calculations and subsequent tangent altitude calculations was carried out by two independent groups, one at Princeton, and the other at GSFC (J. F. Drake, personal communication, 1978) and the final results of tangent ray heights of the two groups agreed to within 0.2 km. A further test was performed in relation to the NO observations (following section) and again the explanation of a systematic phase or altitude shift was found to be entirely unsatisfactory.

The OAO-2 observations of Hays and Roble [4], on the other hand, yield O_3 number densities up to approximately an order of magnitude lower than the model calculations and the data of Gille et al [18]. The OAO-2 O_3 measurements were carried out simultaneously with thermospheric O_2 densities which provide some check on the validity of mesospheric O_3 results. It is not possible to account for the discrepancy by elevating the measured tangent ray height by 10 km. One cannot argue that any one of the O_3 observations reported above are in error. The stellar occultation technique is extremely precise and does not suffer from instrument calibration problems; and the spacecraft attitude and tracking information is known very precisely. Although the photochemistry of mesospheric ozone appears straightforward, it should be re-examined. Perhaps some significant dynamical, physical, or chemical processes including role of excited states have been overlooked in either interpreting the data or in the model calculations.

6. NITRIC OXIDE OBSERVATIONS

Both in 1976 and 1977 Copernicus observations, an attempt was made to determine the NO density from absorption at the $\gamma(1, 0)$ line at 2148.635Å. The 1976 observations were done with a coarser resolution of 0.4Å, with the spectrometer slit centered at λ_0 = 2148.635Å. In 1977, however, a higher resolution, 0.09Å, tube was employed and the line was scanned in each orbit from 2148.238Å to 2148.893Å in steps of $\Delta\lambda$ = 0.046Å. Such scanning would reveal the band structure of $\gamma(1, 0)$ if indeed NO was being measured. Since at 2148Å, O_3, O_2 and Rayleigh scattering also contribute to the total measured optical depth, their contributions had to be subtracted. The O_3 optical depth in the NO line of sight was measured simultaneously at higher wavelengths, while O_2 and Rayleigh scattering contributions were calculated based on the appropriate model atmosphere. The remaining optical depth data were inverted to arrive at the local NO density profile. It was found to be 2×10^8 cm^{-3} at 70 km, or about 100 ppb. This value is about an order of magnitude higher than the daytime observations done by Horvath and Mason [20], and the model predictions (Liu, S. C., personal comm., 1977). For Z>85 km, however, the NO density is found to be $<10^6$ cm^{-3} which is in reasonable agreement with the model predictions of S. C. Liu. A likely explanation for higher NO density is that, after subtracting the contribution of the O_3 optical depth from the total measured optical depth at 2148Å, there may not be any 'band' absorption due to NO left at all, and that the remainder could be continuum absorption due to O_2 and Rayleigh scattering alone.

This, however, requires that the O_2 continuum and Rayleigh scattering absorption be greater than accounted for. If the tangent altitude were in error, this could be accomplished. An exercise was performed in which the tangent altitude was artificially changed by 4 km to check if the remainder absorption was indeed continuum absorption. This is depicted in Fig. 13 where difference between total measured optical depth and measured O_3 optical depth, $\tau_T - \tau_{O_3}$ is plotted against height for orbits 4 and 6 of 1976 and the relevant 1977 orbits. The vertical bars represent the statistical uncertainty. The lower solid line represents the sum of

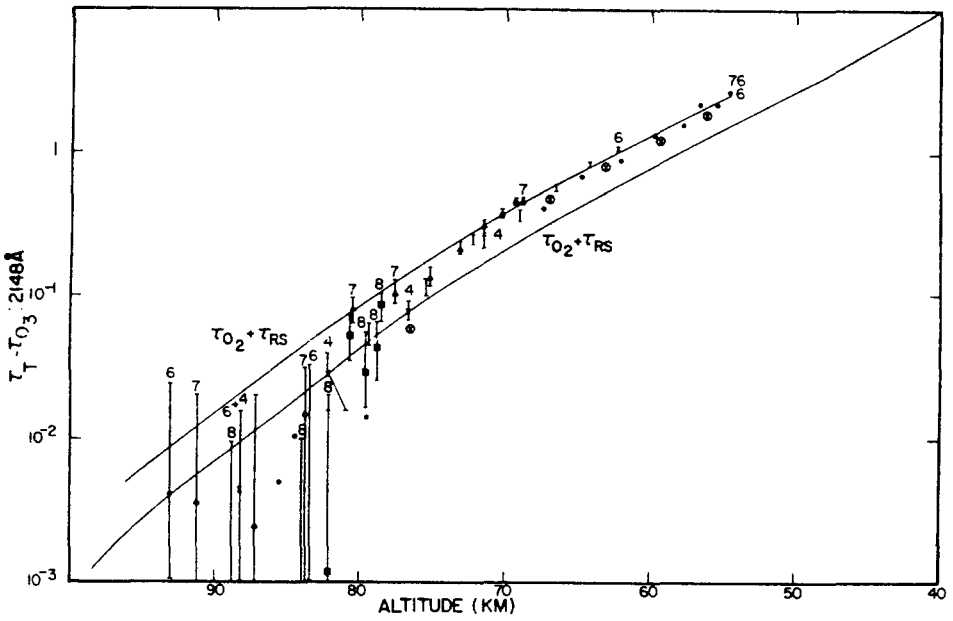

Fig. 13 Total optical depth-optical depth due to O_3 at 2148Å from the Copernicus 1976 and 1977 simultaneous measurements of the selected O_3 and NO wavelengths. The solid lines represent the sum of O_2 and Rayleigh scattering optical depths at the tangent altidue calculated from the spacecraft orbital data, and at an altitude shifted by 4 km.

optical depths of O_2 and that due to Rayleigh scattering, $\tau_{O_2} + \tau_{RS}$ corresponding to the tangent heights of observation. If the altitude calculations were in error, say by 4 km, one would obtain the upper solid line curve for $(\tau_{O_2} + \tau_{RS})$. The upper curve fits the data well up to about 70 km but beyond that there is no fit at all, implying that a systematic error in the tanget height determination could not be responsible for the larger NO and larger O_3 densities obtained by Copernicus measurements. Either there is as yet an unknown absorber in the 2148Å region or there are mesospheric sources of nighttime NO or some dynamical processes which have been overlooked.

7. DISCUSSION

The stellar occultation technique has been successful in determining nighttime height profiles of numberous minor gases which play a major role in the problem of atmospheric pollution and ozone depletion, and also in atomic hydrogen escape. Indeed, this technique provides a means for measuring densities in the region of the atmosphere not generally accessible by balloons, rockets, conventional satellite measurements or ground based optical measurements. The high resolution spectrometer on Copernicus is ideally suited for measuring species with mixing ratios approaching parts per million to parts per billion. The orbital parameters of the IUE spacecraft (Geostationary satellite at 23,000 km altitude) render it undesirable for precision measurements of trace species. The High Resolution Spectrograph on Space Telescope, ST/HRS, on the other hand, can provide spectral and spatial resolution comparable to Copernicus, while the ST sensitivity is a factor of 10 higher. The ST/HRS, furthermore, is an imaging device. These features will make ST the most powerful technique yet developed for measurement of minor gases even less abundant than 0.1 ppb (see Atreya [21]). The pointing and stability characteristics of ST are expected to surpass those of any previous satellites.

8. ACKNOWLEDGMENTS

I am indebted to Thomas M. Donahue for providing insight into the photochemical models and for critically examining the data, and to Paul B. Hays for numerous enlightening discussions about the stellar occcultation technique and about the validity of the data. This research was supported in part by the National Science Foundation Atmospheric Research Section.

9. REFERENCES

1. A. Pannekoek, Astron. Nach., 164, 5 (1903).
2. W. A. Baum and A. D. Code, Astron. J., 58, 108 (1953).
3. P. B. Hays, R. G. Roble and A. N. Shah, Science, 176, 793 (1972).
4. P. B. Hays and R. G. Roble, Planet. Space Sci., 21, 273 (1973).
5. G. R. Riegler, S. K. Atreya, T. M. Donahue, S. C. Liu, B. Wasser and J. F. Drake, Geophys. Res. Lett., 4, 145 (1977).
6. G. R. Riegler, J. F. Drake, S. C. Liu and R. J. Cicerone, J. Geophys. Res., 81, 4997 (1976).
7. S. K. Atreya, T. M. Donahue, W. E. Sharp, B. Wasser, J. F. Drake and G. R. Riegler, Geophys. Res. Lett., 3, 607 (1976).
8. S. K. Atreya, T. M. Donahue and G. R. Riegler. Copernicus Measurements of Ozone in July, 1977. Unpublished data (1980).
9. P. B. Hays and R. G. Roble, Planet. Space Sci., 16, 1197 (1968).
10. S. C. Liu and T. M. Donahue, J. Atmos. Sci., 31, 1118 (1974a).
11. S. C. Liu and T. M. Donahue, J. Atmos. Sci., 31, 1466 (1974b).
12. S. C. Liu and T. M. Donahue, J. Atmos. Sci., 31, 2238 (1974c).
13. P. D. Feldman and P. Z. Takacs, J. Atmos. Sci., 32, 2209 (1975).
14. D. C. Morton and H. L. Dinerstein, Astrophys. J., 204, 1 (1976).
15. K. Watanabe, Advances Geophys., 2, 153 (1958).
16. L. G. Jacchia, Spec. Rep., 332, Smithsonian Astrophys. Obs., Cambridge, MA (1971).
17. T. M. Donahue and G. R. Carignan, J. Geophys. Res., 80, 4565 (1975).
18. J. C. Gille, G. P. Anderson and P. L. Bailey, Geophys. Res. Lett., 7, 525 (1980).
19. A. J. Krueger and R. A. Minzner, J. Geophys. Res., 81, 4477 (1976).
20. J. J. Horvath and C. G. Mason, Geophys. Res. Lett., 5, 1023 (1978).
21. S. K. Atreya, Commentary on p. 72 in "Planetary Astronomy with the Space Telescope," by M. J. S. Belton, Scientific Research with the Space Telescope, U. S. Govt. Printing Office (1979).